Multiple-spin-exchange calculation of the $T=0$ properties of solid ^{3}He

H. Godfrin

AT&T Bell Laboratories, Murray Hill, New Jersey 07974
and Institute Laue-Langevin, 156X 38042 Grenoble Cedex, France

D. D. Osheroff

AT&T Bell Laboratories, Murray Hill, New Jersey 07974

The multiple-exchange Hamiltonian used to describe spin-spin interactions in solid ^{3}He is developed in terms of Pauli spin operators for an arbitrary number of particles in the exchange cycle. The $T=0$ mean-field properties of the "up-up-down-down" (U_2D_2) and canted normal antiferromagnetic magnetic phases are then calculated including two-, three-, four-, five-, and six-particle exchange processes. These properties agree well with experimentally determined melting-curve values when evaluated using the exchange frequencies calculated by Ceperley and Jacucci.

INTRODUCTION

Nuclear magnetic order in solid ^{3}He is believed to be a consequence of the Fermi statistics and exchange of spin-$\frac{1}{2}$ ^{3}He atoms.[1,2] The multiple-spin-exchange model,[1] based on the work by Dirac[3] and Thouless,[4] has been successful in providing a good description of the experimental properties of this system. It is based on the observation[4] that the steric hinderance of the hard cores of the interatomic potentials can favor the coherent exchange of more than two particles. The richness of the observed magnetic phase diagram is understood as the result of competing ferromagnetic and antiferromagnetic interactions, the former being due to exchange of an odd number of particles, and the latter to that of an even number of particles.

Considering only a small number of exchange processes (three- and four-particle exchange), Roger, Delrieu, and Hetherington[1] were able to give a convincing theoretical model for solid ^{3}He. Later work by Roger[5] demonstrated that two-particle exchange was probably as important as three- and planar four-particle exchange. This motivated the development of three-parameter models[6] which allowed an estimation of the exchange frequencies by fitting the experimental database.

Very recently Ceperley and Jacucci[7] determined the frequencies of several exchange processes (up to six spins) using path-integral Monte Carlo techniques. This work confirmed that the most important types of exchange were indeed those considered previously.[1,5,6] However, the frequencies of a large number of other exchange processes were found not to be negligible. It was therefore desirable to calculate the properties of the ordered phases taking into account all these exchange processes. They are calculated at zero temperature in this paper, for the U_2D_2 and the canted normal antiferromagnetic (CNAF) phases.

The ordered phases are described in Sec. I. The multiple-spin-exchange Hamiltonian is given in terms of

Pauli operators in Sec. II. The magnetic properties of the U_2D_2 and CNAF phases are calculated in Sec. III. Section IV is devoted to a comparison with experimental results.

I. THE ORDERED PHASES OF SOLID ^{3}He

The phase diagram of solid ^{3}He on the melting curve, as a function of temperature and magnetic field, is shown in Fig. 1. Three phases have been observed: a paramagnetic phase, the low-field ordered phase, and the high-field ordered phase. These have been described in detail in recent review articles.[1,2]

The structure of the low-field phase is believed to be of the U_2D_2 type, illustrated in Fig. 2. This has been
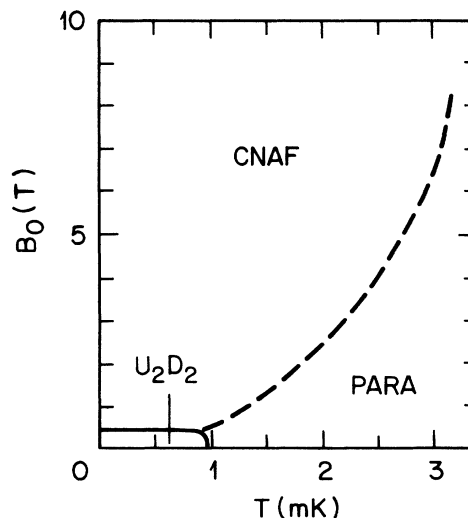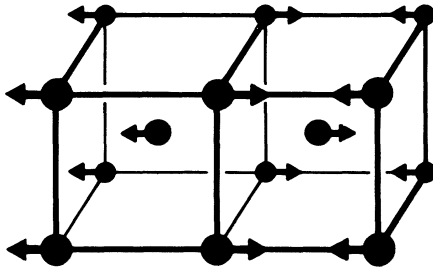

FIG. 1. Experimental phase diagram of melting solid ^{3}He, as a function of temperature and magnetic field, according to Refs. 8, 11, 12, 14, and 15.

FIG. 2. Magnetic structure of the U_2D_2 phase.

demonstrated by Osheroff, Cross, and Fisher[8] using nuclear antiferromagnetic resonance, and confirmed by neutron scattering techniques.[9]

At a magnetic field $B_{c1}=0.451$ T (Ref. 10) (at zero temperature) the system undergoes a first-order transition to the high-field phase. This phase is characterized by a high magnetization slowly dependent on the magnetic field.[10-12] The symmetry of the magnetic lattice is inferred from the NMR lines,[13] which are only shifted by the demagnetizing field.[12,13] The structure is believed to be CNAF (canted normal antiferromagnetic) shown in Fig. 3. This is based on a theoretical analysis supported by the magnetization curve at very high fields.[1,10,11] A transition to the paramagnetic phase at zero temperature is theoretically expected at an upper critical field B_{c2}, where total polarization is achieved. Experimentally, the temperature of the paramagnetic–high-field phase transition is found to increase with field;[11-14] at fields of the order of 7 T, however, it becomes rather constant (~ 3 mK);[11,14] a reentrant phase boundary is therefore possible. The upper critical field at zero temperature, B_{c2}, has been estimated experimentally to be (21.7 ± 1) T.[10] Details on the phase diagram at finite temperatures are given in several review articles[1,13] and in a recent publication.[15]

II. THE MULTIPLE-SPIN-EXCHANGE HAMILTONIAN

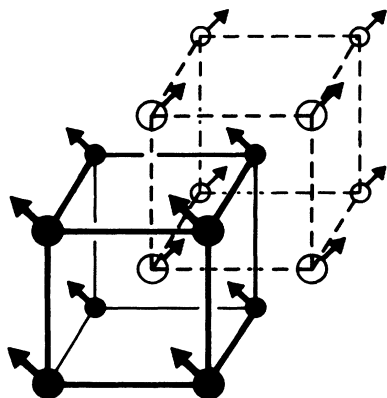The Hamiltonian of N ^{3}He particles (spin $\frac{1}{2}$) in a magnetic field is written as

FIG. 3. Magnetic structure of the CNAF phase.

$$H = H_{ph} + H_x + H_z .\tag{1}$$

The phonon term H_{ph} is not coupled to the exchange (H_x) or to the Zeeman (H_z) terms and is solved separately. The spin-dependent part is hence $H_x + H_z$. The general expression for the exchange Hamiltonian is given by (2), where all $J_{n\alpha}$ are negative[1,4]

$$H_x = \sum_{n,\alpha} J_{n\alpha}(-1)^P \mathcal{P}_n .\tag{2}$$

The summation runs over all the permutations of all the N particles. $\mathcal{P}_n$ is the spin permutation operator of n particles. An exchange coefficient $J_{n\alpha}$ is associated with each permutation $\mathcal{P}_n$ of n particles. The index α distinguishes n-particle cycles which are topologically different (for instance, nearest-neighbor and next-nearest-neighbor exchanges) and obviously have different exchange frequencies. $(-1)^P$ is equal to 1 (-1) for an even (odd) permutation. Since we are considering only cyclic permutations, this corresponds to exchange of an odd (even) number of particles.

For two-particle exchange, $\mathcal{P}_n^{-1}$ is identical to $\mathcal{P}_n$. For n larger than 2, these operators are different, but they must, by symmetry arguments, correspond to the same exchange frequency. It is therefore convenient to write the Hamiltonian as:

TABLE I. Classes of equivalence of $(\sigma_i \cdot \sigma_j)(\sigma_k \cdot \sigma_l)(\sigma_m \cdot \sigma_n)$ elements; heavy lines connect pairs (σ_μ, σ_ν) in the diagrams.

Term type	Diagram	$(-1)^P$	Number of elements
$(\sigma_i \cdot \sigma_j)(\sigma_k \cdot \sigma_l)(\sigma_m \cdot \sigma_n)$		1	2
$(\sigma_i \cdot \sigma_j)(\sigma_k \cdot \sigma_m)(\sigma_l \cdot \sigma_n)$		-1	6
$(\sigma_i \cdot \sigma_l)(\sigma_j \cdot \sigma_n)(\sigma_k \cdot \sigma_m)$		$+1$	3
$(\sigma_i \cdot \sigma_j)(\sigma_k \cdot \sigma_n)(\sigma_l \cdot \sigma_m)$		$+1$	3
$(\sigma_i \cdot \sigma_l)(\sigma_j \cdot \sigma_m)(\sigma_k \cdot \sigma_n)$		-1	1

$$H_x = \sum_{\alpha,n} (-1)^{n+1} J_{n\alpha} \mathcal{P}'_n , \qquad (3)$$

where $\mathcal{P}'_2 = \mathcal{P}_2$ and $\mathcal{P}'_n = (\mathcal{P}_n + \mathcal{P}_n^{-1})$ for $n > 2$. The summation runs over all distinct cycles of n particles and type α. The two-spin permutation operator $\mathcal{P}_2$ (or P_{ij}^σ) has been given by Dirac:[3]

$$P_{ij}^\sigma = (1 + \sigma_i \cdot \sigma_j)/2 , \qquad (4)$$

where the σ_i are the Pauli matrices.

The three- and four-spin permutation operators are obtained as products of two-spin permutation operators.[1,4,16] For three spins

$$P_{ijk}^\sigma = P_{ij}^\sigma P_{ik}^\sigma = \tfrac{1}{4}(1 + \sigma_i \cdot \sigma_j)(1 + \sigma_i \cdot \sigma_k) .$$

Using the identity

$$(\sigma_i \cdot \sigma_j)(\sigma_i \cdot \sigma_k) = \sigma_j \cdot \sigma_k + i\sigma_i \cdot (\sigma_j \times \sigma_k) , \qquad (5)$$

the former expression becomes

$$P_{ijk}^\sigma = \tfrac{1}{4}[1 + \sigma_i \cdot \sigma_j + \sigma_j \cdot \sigma_k + \sigma_k \cdot \sigma_i + i\sigma_i \cdot (\sigma_j \times \sigma_k)] ,$$

and hence

$$\mathcal{P}'_3 = P_{ijk}^\sigma + (P_{ijk}^\sigma)^{-1}$$
$$= \tfrac{1}{2}(1 + \sigma_i \cdot \sigma_j + \sigma_j \cdot \sigma_k + \sigma_k \cdot \sigma_i) \qquad (6)$$

and for four spins

$$\mathcal{P}'_4 = P_{ijkl}^\sigma + (P_{ijkl}^\sigma)^{-1}$$
$$= \tfrac{1}{4}\left[1 + \sum_{\mu < \nu} \sigma_\mu \cdot \sigma_\nu + G_{ijkl}\right] , \qquad (7)$$

where the sum is taken over the six different pairs (μ, ν) among the four particles (i, j, k, l) and

$$G_{ijkl} = (\sigma_i \cdot \sigma_j)(\sigma_k \cdot \sigma_l) + (\sigma_i \cdot \sigma_l)(\sigma_j \cdot \sigma_k)$$
$$- (\sigma_i \cdot \sigma_k)(\sigma_j \cdot \sigma_l) . \qquad (8)$$

Since ring exchanges with five and six particles are considered in this paper, it has been necessary to make similar expansions for the corresponding permutation operators. Using the same techniques, symmetry arguments and patience, the following expressions are obtained. For five spins:

$$\mathcal{P}'_5 = P_{ijklm}^\sigma + (P_{ijklm}^\sigma)^{-1}$$
$$= \frac{1}{2^3}\left[1 + \sum_{\mu < \nu} \sigma_\mu \cdot \sigma_\nu + \sum_{\mu < \nu < \eta < \epsilon} G_{\mu\nu\eta\epsilon}\right] . \qquad (9)$$

The first sum is taken over the ten different pairs (μ, ν), and the second sum over the five combinations of four spins among the five-spin cycle. The expression of G is given by formula (8).

For six spins,

$$P_6' = P_{ijklmn}^\sigma + (P_{ijklmn}^\sigma)^{-1}$$
$$= \frac{1}{2^4}\left[1 + \sum_{\mu < \nu} \sigma_\mu \cdot \sigma_\nu + \sum_{\mu < \nu < \eta < \epsilon} G_{\mu\nu\eta\epsilon} + S_{ijklmn}\right] , \qquad (10)$$

where

$$S_{ijklmn} = [(\sigma_i \cdot \sigma_j)(\sigma_k \cdot \sigma_l)(\sigma_m \cdot \sigma_n) + (\sigma_j \cdot \sigma_k)(\sigma_l \cdot \sigma_m)(\sigma_n \cdot \sigma_i)]$$
$$- [(\sigma_i \cdot \sigma_j)(\sigma_k \cdot \sigma_m)(\sigma_l \cdot \sigma_n) + (\sigma_j \cdot \sigma_k)(\sigma_l \cdot \sigma_n)(\sigma_m \cdot \sigma_i) + (\sigma_k \cdot \sigma_l)(\sigma_m \cdot \sigma_i)(\sigma_n \cdot \sigma_j)$$
$$+ (\sigma_l \cdot \sigma_m)(\sigma_n \cdot \sigma_j)(\sigma_i \cdot \sigma_k) + (\sigma_m \cdot \sigma_n)(\sigma_i \cdot \sigma_k)(\sigma_j \cdot \sigma_l) + (\sigma_n \cdot \sigma_i)(\sigma_j \cdot \sigma_l)(\sigma_k \cdot \sigma_m)]$$
$$+ [(\sigma_i \cdot \sigma_l)(\sigma_j \cdot \sigma_n)(\sigma_k \cdot \sigma_m) + (\sigma_j \cdot \sigma_m)(\sigma_k \cdot \sigma_i)(\sigma_l \cdot \sigma_n) + (\sigma_k \cdot \sigma_n)(\sigma_l \cdot \sigma_j)(\sigma_m \cdot \sigma_i)]$$
$$+ [(\sigma_i \cdot \sigma_j)(\sigma_k \cdot \sigma_n)(\sigma_l \cdot \sigma_m) + (\sigma_j \cdot \sigma_k)(\sigma_l \cdot \sigma_i)(\sigma_m \cdot \sigma_n) + (\sigma_k \cdot \sigma_l)(\sigma_m \cdot \sigma_j)(\sigma_n \cdot \sigma_i)]$$
$$- [(\sigma_i \cdot \sigma_l)(\sigma_j \cdot \sigma_m)(\sigma_k \cdot \sigma_n)] . \qquad (11)$$

This can be written in a more compact form:

$$S_{ijklmn} = \sum_{C(i,j,k,l,m,n)} (-1)^P (\sigma_\alpha \cdot \sigma_\beta)(\sigma_\gamma \cdot \sigma_\delta)(\sigma_\epsilon \cdot \sigma_\phi) .$$

The sum is taken over the 15 combinations of (i, j, k, l, m, n) in three different pairs. $(-1)^P$ is 1 for the cyclic combinations. There are two of them, given by the first term (within brackets) in formula (11), and they can be represented by diagram 1 of Table I. $(-1)^P$ is -1 (1) if a combination is obtained by an odd (even) number of transpositions between different pairs. For instance, the six combinations given by the second term (within brack-

ets) in formula (11) are obtained by $2n + 1$ transpositions from the cyclic combination. These are represented by diagram 2 in Table I. Similar arguments explain the other diagrams of Table I.

More rigorously, the products $(\sigma_\alpha \cdot \sigma_\beta)(\sigma_\gamma \cdot \sigma_\delta)(\sigma_\epsilon \cdot \sigma_\phi)$ are grouped in classes of equivalence. Elements in the same class are connected by the cyclic permutation. A new class is obtained by applying transpositions between different pairs of any element and then the cyclic permutation to cover the whole class. The sign $(-1)^P$ is given by the parity of the class of equivalence. This is also verified, obviously, for the four-spin operator G_{ijkl}.

These very simple rules govern the generation of

higher-order terms in the expansion of the permutation operators in terms of Pauli matrices. It is straightforward to derive similar expansions for seven, eight, or more spin cycles.

III. MULTIPLE EXCHANGE IN bcc SOLID ^{3}He

A. Exchange cycles

The multiple-spin-exchange Hamiltonian involves a sum over all the possible permutations of the N particles. However, only some permutations including a limited number of particles are supposed to have significant probability.[5,7] The exchange cycles considered here are listed in Table II and shown in Fig. 4. The number of cycles of

each type found in a bcc lattice with N atoms has been computed by group theory techniques, using the translational and point group symmetry of the lattice, and the symmetry of each cycle to ensure that a given cycle is only counted once.

The notation used by McMahan and Guyer[16] provides an excellent description of the exchange cycles, but it is not adequate in the context of calculations. A more compact notation has been used in this work, described in Table II.

B. Alternative expressions for the Hamiltonian

For the exchanges considered here the Hamiltonian (2) is

$$
\begin{aligned}
H_x = \sum_\alpha & \left[-\tfrac{1}{2} \sum_{i<j} J_{\alpha N}(1+\sigma_i\cdot\sigma_j) + \tfrac{1}{2} \sum_{(ijk)} T_\alpha(1+\sigma_i\cdot\sigma_j+\sigma_j\cdot\sigma_k+\sigma_k\cdot\sigma_i) \right. \\
& -\tfrac{1}{4} \sum_{(ijkl)} K_\alpha \left[1+ \sum_{\mu<\nu} \sigma_\mu\cdot\sigma_\nu + G_{ijkl} \right] + \tfrac{1}{8} \sum_{(ijklm)} F_\alpha \left[1+ \sum_{\mu<\nu} \sigma_\mu\cdot\sigma_\nu + \sum_{\mu<\nu<\eta<\epsilon} G_{\mu\nu\eta\epsilon} \right] \\
& \left. -\tfrac{1}{16} \sum_{(ijklmn)} S_\alpha \left[1+ \sum_{\mu<\nu} \sigma_\mu\cdot\sigma_\nu + \sum_{\mu<\nu<\eta<\epsilon} G_{\mu\nu\eta\epsilon} + S_{ikjlmn} \right] \right] .
\end{aligned}
\tag{12}
$$

It is convenient, for the calculation of some properties, to write this Hamiltonian as

$$
H_x = -\frac{J_1}{2} \sum_{i<j}^{(1)} \sigma_i\cdot\sigma_j - \frac{J_2}{2} \sum_{i<j}^{(2)} \sigma_i\cdot\sigma_j \cdots - \frac{J_k}{2} \sum_{i<j}^{(k)} \sigma_i\cdot\sigma_j - \cdots + O(\sigma^4) + O(\sigma^6) .
\tag{13}
$$

The constant term has been omitted for clarity; the terms of order σ^4 [i.e., of the form $(\sigma_i\cdot\sigma_j)(\sigma_k\cdot\sigma_l)$] and order σ^6 can be easily obtained; they will not be needed in this paper. The superscript on the summation symbol indicates that sums are taken over nearest neighbor (1), second-neighbor (2) pairs. The J_k obviously contain contributions of J_{kN}, but also from T_α, K_α, F_α, S_α, etc. For instance, the exchange T_1 requires exchange of two nearest-neighbor pairs and a next-nearest-neighbor pair.

Using the number of cycles of each type and the number of neighbors of each type (see Table II) it can be readily shown that

TABLE II. Type and number of exchange cycles.

| Exchange type	This work	Notation Ref. 1	Refs. 16 and 7	Number of cycles
Nearest-neighbor	J_{1N}	J_{NN}	(1)	$4N$
Second	J_{2N}	J_{NNN}	(2)	$3N$
Third	J_{3N}		(3)	$6N$
Fourth	J_{4N}		(4)	$12N$
Fifth	J_{5N}		(5)	$4N$
Sixth	J_{6N}		(6)	$3N$
Seventh	J_{7N}		(7)	$12N$
Triangular 1	T_1	J_t	(112)	$12N$
Triangular 2	T_2		(113)	$12N$
Four-spin planar	K_P	K_P	$(1^4;23)$	$6N$
Four-spin folded	K_F	K_F	$(1^4;22)$	$6N$
Four-spin diamond	K_A		(1122;31)	$24N$
Four-spin eight	K_B		(1212;11)	$12N$
Four-spin lozenge	K_L		(1212;14)	$12N$
Four-spin square	K_S		$(2^4;33)$	$3N$
Five spin	F		$(1^42;52341)$	$24N$
Six-spin crown	S_1		$(1^6;3^6;4^3)$	$4N$
Six-spin planar	S_2		$(1^6;523523;417)$	$12N$
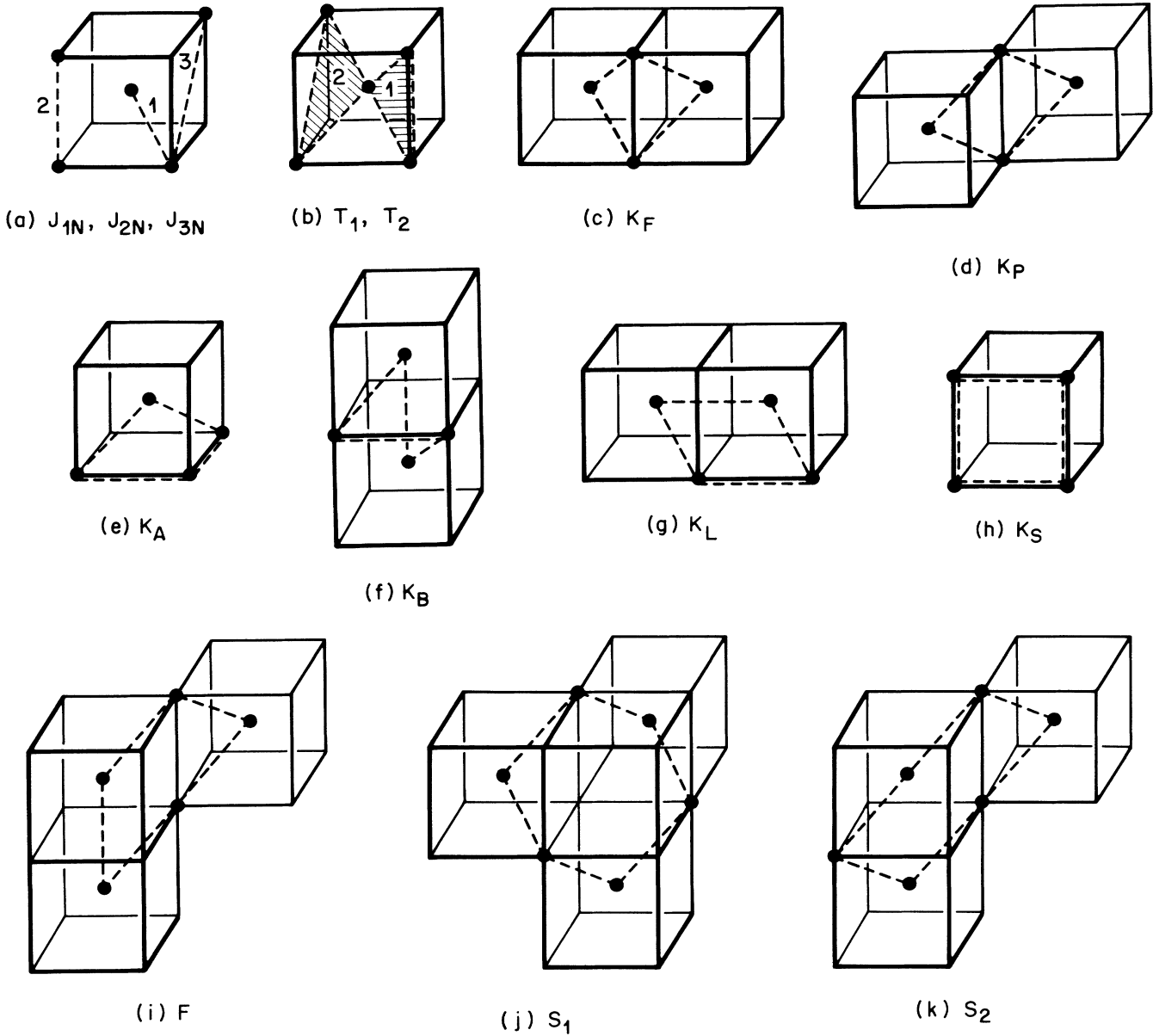
FIG. 4. Type of exchange cycles considered in the bcc lattice. (a) Two-particle exchange; 1: nearest neighbors; 2: second neighbors; 3: third neighbors. (b) Three-particle exchange; 1: $T_1(112)$; 2: $T_2(113)$. (c) Folded four-spin exchange K_F. (d) Planar four-spin exchange K_P. (e) Diamond four-spin exchange K_A. (f) Eight four-spin exchange K_B. (g) Lozenge four-spin exchange K_L. (h) Square four-spin exchange K_S. (i) Five-spin exchange F. (j) Crown six-spin exchange S_1. (k) Planar six-spin exchange S_2.

$$J_1 = J_{1N} - 6T_1 - 6T_2 + 3K_F + 3K_P + \tfrac{9}{2}K_L + 9K_A + 6K_B - \tfrac{15}{2}F + \tfrac{3}{4}S_1 + \tfrac{21}{8}S_2 \ ,$$

$$J_2 = J_{2N} - 4T_1 + 2K_F + K_P + 8K_A + 4K_B + 4K_L + 2K_S - 4F + S_2 \ ,$$

$$J_3 = J_{3N} - 2T_2 + \frac{K_P}{2} + 2K_A + \frac{K_S}{2} - F + \frac{S_1}{2} + \frac{S_2}{2} \ , \tag{14}$$

$$J_4 = J_{4N} + \frac{K_L}{2} + \frac{S_1}{8} - \frac{F}{2} + \frac{S_2}{8} \ ,$$

$$J_5 = J_{5N} - \tfrac{3}{2}F + \tfrac{3}{4}S_2, \quad J_6 = J_{6N}, \quad J_7 = J_{7N} + \frac{S_2}{8} \ .$$

It should be noted that the sign of $J_{\alpha N}$, T_α, K_α, S_α is negative; the J_k can be either positive or negative.

C. Magnetic properties of the paramagnetic phase

Although the finite-temperature properties are not studied in this paper, it is straightforward to derive the expression for the Curie-Weiss temperature Θ_W as a function of the exchange parameters. Only the quadratic terms in the spin variable σ of the exchange Hamiltonian contribute to Θ_W (see, for instance, Ref. 1). Using the expression 13 for the Hamiltonian and the number of cycles (pairs) of each type (given in Table II) for the bcc lattice the following result is obtained:

$$\Theta_W = 4J_1 + 3J_2 + 6J_3 + 12J_4 + 4J_5 + 3J_6 + 12J_7 \tag{15}$$

which can be written in terms of exchange coefficients as

$$\Theta_W = 4J_{1N} + 3J_{2N} + 6J_{3N} + 12J_{4N} + 4J_{5N} + 3J_{6N} + 12J_{7N} - 36T_1 - 36T_2$$

$$+ 18K_F + 18K_P + 36K_L + 72K_A + 36K_B + 9K_S - 60F + \tfrac{15}{2}S_1 + \frac{45}{2}S_2 \ . \tag{16}$$

It should be noted that the compensation of terms with different signs may be important. Moreover, exchange processes involving a large number of atoms are expected to have small probabilities, but they are weighed by a larger factor than two or three spin-exchange coefficients and can have substantial contributions to Θ_W.

D. Magnetic properties of the CNAF phase at zero temperature

The N spins are located on two interpenetrating cubic sublattices (noted A and B) which are supposed to be fully polarized at absolute zero. The magnetic induction $\mathbf{B}_0$ is chosen to be in the z direction. The angle between $\mathbf{B}_0$ and the sublattices magnetization is θ. Hence, the reduced magnetization of the system is $m = M/M_{sat} = \cos\theta$; the saturation magnetization is $M_{sat} = \tfrac{1}{2}\hbar\gamma(N/V)$, γ the gyromagnetic ratio of the ^{3}He nucleus, and V the volume of the system.

The mean value of the energy can be calculated neglecting fluctuations using the approximation[1]

$$\langle \sigma_i \cdot \sigma_j \rangle \simeq \langle \sigma_i \rangle \cdot \langle \sigma_j \rangle \ ,$$

the expression (12) for the exchange Hamiltonian, and the Zeeman Hamiltonian

$$H_Z = -\sum_i \frac{\gamma}{2}\hbar\sigma_i \cdot \mathbf{B} \ .$$

The evaluation of the expectation values of the products of Pauli operators is simplified by the symmetry of the magnetic lattice. For instance, if a spin in sublattice A is considered, the first neighbor will be in sublattice B, the second neighbor in A, etc., . . . ; this is summarized in Table III. Therefore, the terms of the form $\sum(\sigma_i \cdot \sigma_j)$ will provide a magnetization dependence of the energy only when σ_i and σ_j are first, fourth, seventh, etc., neighbors.

Calculation of the sums involved in four- and six-particle operators require one to find and classify the quadruplets and sextuplets according to their spin configurations. In the CNAF phase all cycles of a given type (e.g., K_F, K_P, etc.) have the same spin configuration irrespective of their position or orientation in the lattice. It is therefore straightforward to construct classification tables (available on request) which allow a direct evalua-

tion of $\langle H \rangle$ in the high-field (CNAF) phase, noted as $\langle H \rangle_H$, in terms of the reduced magnetization $m_H = \cos\theta$

$$\frac{\langle H \rangle_H}{Nk_B} = a + bm_H^2 + cm_H^4 + dm_H^6 - \frac{\gamma\hbar}{2k_B}m_H B_0 \ ,$$

with

$$a = (-3J_{2N} - 6J_{3N} - 4J_{5N} - 3J_{6N} - 6K_S) \ ,$$

$$b = 4(-J_{1N} - 3J_{4N} - 3J_{7N} + 6T_1 + 6T_2$$
$$\quad - 12K_A - 6K_B - 6K_L) \ ,$$

$$c = 12(-K_P - K_F + 4F) \ , \tag{17}$$

$$d = 8(-S_1 - 3S_8) \ ,$$

and $k_B/\gamma\hbar = 0.6424$ T/mK. Minimizing the energy with respect to the magnetization leads to a simple result for the zero-temperature magnetization curve $m_H(B_0)$:

$$B_0 = \frac{4k_B}{\gamma\hbar}(bm_H + 2cm_H^3 + 3dm_H^5) \ . \tag{18}$$

The upper critical field B_{c2} corresponds to total polarization ($m_H = 1$):

$$B_{c2} = \frac{4k_B}{\gamma\hbar}(b + 2c + 3d) \ , \tag{19}$$

TABLE III. Neighbors of an atom in sublattice A in the CNAF phase (a is the lattice parameter).

Neighbor	Sublattice	Distance
First	B	$a\sqrt{3}/2$
Second	A	a
Third	A	$a\sqrt{2}$
Fourth	B	$a\sqrt{11}/2$
Fifth	A	$a\sqrt{3}$
Sixth	A	$2a$
Seventh	B	$a\sqrt{19}/2$
Eighth	A	$a\sqrt{5}$

$$B_{c2} = \frac{16k_B}{\gamma\hbar}(-J_{1N} -3J_{4N} +6T_1 +6T_2 -3K_P -3K_F$$

$$+12F -12K_A -6K_B -6K_L -2S_1 -6S_2) ,$$

(20)

and the magnetization of the CNAF phase at zero field is m_0:

$$m_0^2 = m_H^2(B_0=0) = \frac{c}{3d}\left[-1+\left[1-3\frac{bd}{c^2}\right]^{1/2}\right] ,$$

(21)

when b is negative and c and d are positive as observed experimentally.[10] This spontaneous magnetization at zero field is not directly observed in practice since this system undergoes a first-order transition to the U_2D_2 phase. However, the low value of B_{c1} allows an accurate extrapolation of m_H to $B_0=0$.[10] This "pseudoferromagnetic" phase has been predicted in earlier works (see Ref. 1 and references therein) which considered four spin (K_F or K_P) exchange.

The expression derived here includes several types of exchange not considered in Ref. 1. The main effect is a renormalization of the terms a, b, and c in the expression of the energy, and the introduction of a new term (d). As will be shown later on, these corrections are important, and dominate the magnetic behavior of the CNAF at high polarization ($m \simeq 1$).

The main interest in the multiple-spin-exchange model, however, results from the fact that only a limited number of terms in the expansion of the energy in powers of m [Eq. (17)] is expected to be important. It is obvious from the preceding calculations that the coefficient of the m^i term will contain contributions from exchange cycles involving $j \geq i$ particles. Since the exchange frequencies are expected to decrease rapidly as a function of j (at least for relatively large rings),[5] the major contribution to the coefficient of m^i will come from rings of i particles. Among these, rings of i nearest neighbors are expected to dominate:[5] cm^4 is dominated by K_P and K_F, dm^6 by S_1 and S_2, etc.

In the CNAF phase, nearest neighbors are on different sublattices. The Hamiltonian (12) has the following important property: The contribution to the energy of an exchange of n nearest-neighbor particles, where n is any even number of particles and J_n the corresponding exchange frequency, is

$$\langle H \rangle_n = Nk_B 2J_n\cos^n\theta = 2Nk_B J_n m^n$$

(for two particles it is $Nk_B J_{NN}\cos^2\theta$ due to the definition of J). Therefore, K_F and K_P only contribute to the m^4 term, S_1 and S_2 to the m^6, etc.

Of course, higher-order exchanges will renormalize these coefficients. It should be kept in mind, however, that exchange processes with an odd number of particles necessarily contain 2^d neighbors (or even more distant ones), and their frequency is expected to be much smaller than that of smaller rings of nearest neighbors. Therefore, for sufficiently large i, the coefficients of m^i in the expression of the energy must be positive.

Hence, a term in m^8 due to eight or more spin ex-

changes is expected to be much smaller than dm^6, and positive. This general discussion obviously does not apply for the first terms in the expansion which contain contributions of small rings; the coefficients a and b, for instance, are renormalized by a large number of exchange processes [see Eq. (17)] and even their sign cannot be inferred a priori.

The magnetization curve in the CNAF phase [Eq. (18)] results from a simple combination of these coefficients, and provides a direct probe of the relative importance of the various exchange processes; this point will be discussed further in Sec. IV.

E. Magnetic properties of the U_2D_2 phase

The magnetic properties of the U_2D_2 phase are more difficult to evaluate than those of the CNAF phase studied in the preceding section. Because of the lower symmetry, the spin configuration of a particular ring of i spins will depend on the position and on the orientation of the ring in the lattice. To perform the sums over all the cycles involved in the exchange Hamiltonian, the spin configurations for each type of cycle have been classified and counted; for example, there are 24 quadruplets of the type $A A AB$ per S_2 exchange cycle in the U_2D_2 phase (the tables are available on request).

Two of the four sublattices contain spins totally aligned in a direction which makes an angle θ with the magnetic field B_0 (spins of type A), and the other two sublattices contain spins totally aligned, with the same angle and symmetric with respect to B_0 (spins of type B). The angle between spins A and B is therefore 2θ. The reduced magnetization of the U_2D_2 (low-field) phase is $m_L = \cos\theta$. Using the classification of the spin configurations the mean value of the energy is obtained easily:

$$\frac{\langle H \rangle_L}{Nk_B} = u +vm_L^2 +wm_L^4 -\frac{\gamma\hbar}{2k_B}m_LB_0 ,$$

with

$$u = -(2J_{1N} +2J_{2N} +2J_{3N} + \cdots -8T_1$$

$$-4T_2 +2K_F +8K_A +4K_B +8K_L +2K_S) ,$$

$$v = -(2J_{1N} +J_{2N} +4J_{3N} + \cdots -16T_1$$

$$-20T_2 +12K_P +8K_F +40K_A +20K_B$$

$$+16K_L +4K_S -36F +4S_1 +12S_2) ,$$

(22)

$$w = -(2K_F -12F +4S_1 +12S_2) .$$

The magnetization curve $m_L(B_0)$ is obtained by minimizing the energy with respect to m_L:

$$B_0 = \frac{4k_B}{\gamma\hbar}(vm_L +2wm_L^3) .$$

(23)

According to this formula, the magnetization in the U_2D_2 phase is not linear in magnetic field. For low values of m_L (low fields), $B_0 \simeq (4k_B/\gamma\hbar)vm_L$.

Since $m_L = M/M_{sat}, M_{sat} = (N/V)(\gamma\hbar/2)$, and the sus-

ceptibility $\chi = \mu_0 M / B_0$ (where $\mu_0 = 4\pi 10^{-7}$), then

$$\chi \simeq C / T^* = \mu_0 N \left[\frac{\gamma \hbar}{2} \right]^2 / (2 v V k_B) \qquad (24)$$

with $T^* = 2v$; C is the Curie constant.

It has been assumed that v is positive; otherwise the $U_2 D_2$ phase would have a spontaneous magnetization (as in the CNAF case), and would not be the stable phase at $B_0 = 0$.

F. Energy difference between the CNAF and $U_2 D_2$ phases

The difference of the energies between the two phases at zero field is given by formulas (17), (21), and (22), and should be positive:

$$\frac{\langle E \rangle_H}{N k_B} - \frac{\langle E \rangle_L}{N k_B} = a + b m_0^2 + c m_0^4 + d m_0^6 - u \ . \qquad (25)$$

The difference of the energies should vanish at the lower critical field B_{c1}. Equating expressions (17) and (22), and using the magnetization curves [expressions (18) and (23)] one obtains an implicit equation for B_{c1}, which can be solved numerically for a given set of exchange frequencies.

G. Exchange frequencies

The exchange frequencies for the processes studied here have been calculated by Ceperley and Jacucci[7] using path-integral Monte Carlo techniques. Their latest[17] results are summarized in Table IV, after scaling with a Grüneisen parameter $\Gamma = \partial \log J / \partial \log V \simeq 18$, for $V = 24.22$ cm^3, the molar volume at melting pressure and low temperatures. This correction is small (7.5%), and the exact value of Γ is not important within present error bars.

IV. CALCULATION OF THE MAGNETIC PROPERTIES OF bcc ^{3}He ON THE MELTING CURVE

Most of the experiments at very low temperatures have been performed with solid ^{3}He on the melting curve; it is therefore particularly interesting to calculate the magnetic properties with the equations derived in the preceding section and the exchange coefficients calculated by Ceperley and Jacucci.[7]

A. CNAF phase (on the melting curve)

From Eq. (17), the coefficients of the energy expansion are

$$a = (0.213 \pm 0.015) \text{ mK} \ ,$$
$$b = (-2.21 \pm 0.27) \text{ mK} \ ,$$
$$c = (3.56 \pm 0.20) \text{ mK} \ , \qquad (26)$$
$$d = (0.555 \pm 0.069) \text{ mK} \ .$$

The magnetization curve is given by the expression

$$B_0 = (-5.7 \pm 0.7) m_H + (18.3 + 1) m_H^3 + (4.3 \pm 0.5) m_H^5 \ , \qquad (27)$$

where B_0 is given in T. Therefore, the upper critical field is

$$B_{c2} = (16.9 \pm 1.4) \text{ T} \ , \qquad (28)$$

and the reduced magnetization at zero field m_0 is

$$m_0 = (0.54 \pm 0.05) \ . \qquad (29)$$

It is approximately equal, within this range of parameters, to $(-b/2c)^{1/2}$.

The experimental values for these quantities are[10]

$$B_0 = (-9.1 \pm 0.6) m_H + (23.8 \pm 2) m_H^3 + (7.6 \pm 2) m_H^5 \text{ T} \ ,$$
$$B_{c2} = (22.3 \pm 0.4) \text{ T} \ , \qquad (30)$$

TABLE IV. Exchange frequencies from Ref. 7, scaled to 24.22 cm^3/mole.

	Type of exchange		Exchange frequency (mK)
2	J_{1N}	(1)	-0.487 ± 0.015
2	J_{2N}	(2)	-0.067 ± 0.005
3	T_1	(112)	-0.193 ± 0.010
3	T_2	(113)	-0.0057 ± 0.0009
4	K_P	$(1^4, 23)$	-0.269 ± 0.016
4	K_F	$(1^4; 22)$	-0.034 ± 0.004
4	K_A	(1122; 31)	-0.0065 ± 0.0016
4	K_B	(1212; 11)	-0.00054 ± 0.00025
4	K_L	(1212; 14)	-0.012 ± 0.0035
4	K_S	$(2^4; 33)$	-0.0020 ± 0.0006
5	F	$(1^4 2; 52341)$	-0.0016 ± 0.0002
6	S_1	$(1^6; 3^6; 4^3)$	-0.037 ± 0.008
6	S_2	$(1^6; 523523; 417)$	-0.0108 ± 0.0011

and $m_0 = (0.587 \pm 0.002)$ when fitting the magnetization curve to Eq. (17). For several other types of fit, $B_{c2} = (21.7 \pm 1)$ T and $m_0 = (0.583 \pm 0.006)$. The results of the present calculation and the experimental values of Ref. 10 are shown in Fig. 6. Clearly, the agreement between theory and experiment is good. The sign and the magnitudes of the coefficients of the expression for the magnetization are correct. There is, however, a systematic tendency toward lower theoretical values. The fact that m_0 (essentially the ratio of exchange frequencies) is correctly predicted indicates that all exchange frequencies could be systematically underestimated.

Theory and experiment are consistent (within error bars) is all exchange frequencies are increased by 37% (Fig. 5). However, such a large discrepancy is not consistent with the excellent agreement between theory and experiment in the paramagnetic phase (see Sec. IV C and Ref. 7). Furthermore, it is far outside combined experimental and theoretical error bars.

There is a simple alternative explanation. It should be noted that the magnetization curve can be written as

$$B_0 = \sum_{i=0}^{\infty} x_{2i+1} m^{2i+1}$$

when all exchange processes are considered. Within the limited subset of cycles considered here, $B_0 = x_1' m + x_3' m^3 + x_5' m^5$, and the analysis of the experimental data of Ref. 10 was performed imposing this functional form. It is possible that higher-order exchange cycles, although having relatively low frequencies, are so numerous that their overall contribution is not negligible.[2] This would give rise to two effects: First, the coefficients would be renormalized (i.e., $x_i' \neq x_i$), and second, higher-order terms (x_{2i+1} with $i > 2$) would contribute. The renormalization of the coefficients is difficult
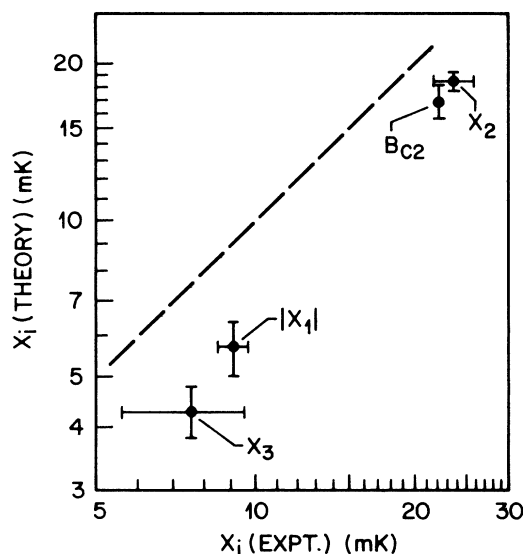

FIG. 5. The x_i coefficients of the magnetization curve $B_0 = x_1 m + x_2 m^3 + x_3 m^5$ and $B_{c2} = x_1 + x_2 + x_3$, determined theoretically (this work) compared to the experimental values (Ref. 10) of Osheroff, Godfrin, and Ruel.

to evaluate. The expression of the coefficients b and c [Eq. (17)] suggests that renormalization tends to reduce the magnitude of the coefficients (therefore making the discrepancy worse), and that this effect is small.

The contribution of higher-order terms can in principle reconcile theory and experiment. As shown previously, these terms have positive coefficients x_{2i+1} for $i \geq 1$. The experimental estimate of B_{c2} (Ref. 10) indicates that

$$\sum_{i=3}^{\infty} x_{2i+1} \simeq 5 \text{ T } .$$

The relatively slow decrease of these coefficients ($x_3 = 18.3$; $x_5 = 4.3$ T) suggests that this is indeed possible. A theoretical calculation of x_7 would be a crucial test: If $x_7 \sim 1$ T, the above condition can be fulfilled. Since the major contribution to x_7 should come from rings of eight nearest neighbors, the calculation can be limited to only a few new exchange cycles.

The high-order terms are only important at very high fields, near B_{c2}, where an almost complete polarization of the spins is achieved ($m \simeq 1$). Experiments in this field range can bring an experimental answer to this problem.

B. $U_2 D_2$ phase (on the melting curve)

From Eq. (22), the coefficients of the energy expansion are

$$u = (-0.237 \pm 0.092) \text{ mK },$$
$$v = (+2.03 \pm 0.27) \text{ mK },$$
$$w = (+0.326 \pm 0.036) \text{ mK }.$$

(31)

The magnetization curve $m_L(B_0)$ is given by the expression

$$B_0(\text{T}) = (5.2 \pm 0.7) m_L + (1.7 \pm 0.2) m_L^3 .$$

(32)

For small magnetizations (i.e., small B_0) the susceptibility is $X = \mu_0(M/B_0) = (C/T^*)$, C is the Curie constant, $2.613 \, 04 \times 10^{-7}$ (mks) for $V = 24.22$ cm^3/mol, and $T^* = 2v$

$$T^* = (4.06 \pm 0.54) \text{ mK }.$$

It should be noted that for magnetizations smaller than a tenth of the saturation value ($m_L < 0.1$), m_L is linear in field within 0.3%, and this phase can be described by a constant susceptibility

$$X = (6.44 \pm 0.85) \times 10^{-5} \text{ (mks)}$$
$$= (5.12 \pm 0.68) \times 10^{-6} \text{ (cgs)}$$

(see Figs. 6 and 7).

The experimental values for these quantities are given in Ref. 10. The largest value of m_L observed in the $U_2 D_2$ phase is 9.14% of the saturation magnetization. According to the previous calculation only very small departures from a linear law are expected in $m_L(B_0)$ for these small values of m_L. The experiment confirms the linearity within error bars $\simeq 3\%$.

The measured susceptibility is $X = (5.41 \pm 0.08) \times 10^{-6}$ (cgs), and therefore $T^* = (3.84 \pm 0.06)$ mK, in good agree-
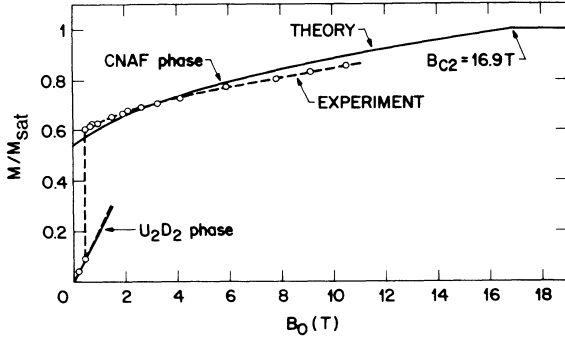
FIG. 6. Zero-temperature magnetization of solid ^{3}He (normalized to the saturation magnetization) as a function of magnetic field, for a molar volume of 24.22 cm^3. The open circles connected by dashed lines are the experimental values determined by Osheroff, Godfrin, and Ruel (Ref. 10). The results of the present calculations are indicated by solid lines.

ment with the theoretical values. This is particularly surprising, since the theory neglects zero-point spin fluctuations. According to theoretical estimates,[1,2] the susceptibility should be reduced by approximately 20% from its predicted value.

It should be noted that if, as suggested after the analysis of the CNAF phase, the exchange constants were underestimated by 37%, then a large disagreement between the calculations and experiment would result here, for the U_2D_2 phase. Moreover, correction for quantum fluctuations would make the discrepancy even worse.

C. Paramagnetic phase (on the melting curve)

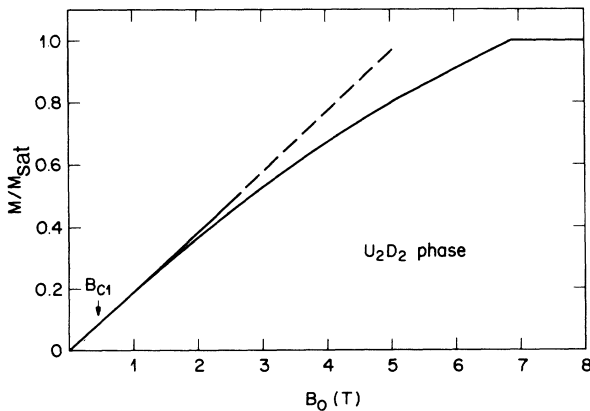According to formula (16), the Curie-Weiss temperature on the melting curve is

FIG. 7. The calculated magnetization of the U_2D_2 phase as a function of the magnetic field. Note that deviations from linearity are small for fields $< B_{c1}$, where the U_2D_2 phase is stable.

$$\Theta_W = 4J_{1N} + 3J_{2N} - 36T_1 - 36T_2 + 18K_F + 18K_P + 36K_L$$
$$+ 72K_A + 36K_B + 9K_S - 60F + 7.5S_1 + 22.5S_2 ,$$
(33)

where only the terms with known exchange frequencies have been retained.

Therefore $\Theta_W = (-1.81 \pm 0.5)$ mK. The cancellation of terms of opposite sign and their magnitude is sketched in Fig. 8. Surprisingly, the value of Θ is of the order of $4J_{1N}$, the first term in the series, due to an almost exact cancellation of the following terms. It should be noted that even if J_{1N}, T_1, and K_P are the leading terms, several others have to be considered to obtain a moderately accurate value of Θ_W.

The calculated value has the right sign and magnitude according to recent experiments;[18] $\Theta_W = -(1.8 \pm 0.1)$ mK. It has to be pointed out, however, that this value is substantially lower in magnitude than that found in earlier NMR experiments.

The coefficients J_i in the expression (13) for the Hamiltonian can be calculated as a function of the exchange frequencies using the formula (14):

$$J_1 = (-0.364 \pm 0.082) \text{ mK} ,$$

$$J_2 = (+0.257 \pm 0.048) \text{ mK} ,$$

$$J_3 = (-0.159 \pm 0.010) \text{ mK} ,$$

$$J_4 = (-0.011 \pm 0.002) \text{ mK} ,$$

$$J_5 = (-0.0057 \pm 0.001) \text{ mK} ,$$

$$J_6 = 0 ,$$

$$J_7 = (-0.0014 \pm 0.000\,14) \text{ mK} .$$

These are often more convenient for calculating thermodynamic properties of ^{3}He in the paramagnetic phase.

Ceperley and Jacucci[7] have calculated several important parameters of the high-temperature expansions of the susceptibility and the specific heat (including the Curie-Weiss temperature also derived here). The agreement with experimental quantities is good.

D. Calculation of the energy

The energy of the ordered phases is calculated in this section with the exchange constants of Table IV, i.e., for melting solid ^{3}He. The exchange Hamiltonian (12) has a constant (spin independent) term; therefore the energy per particle of free spins at $T = 0$ is not zero, but

$$E_0 = -(2J_{1N} + \tfrac{3}{2}J_{2N} - 6T_1 - 6T_2 + \tfrac{3}{2}K_F + \tfrac{3}{2}K_P + 6K_A$$
$$+ 3K_B + 3K_L + \tfrac{3}{4}K_S - 3F + \tfrac{1}{4}S_1 + \tfrac{3}{4}S_2) . \quad (34)$$

At melting density, $E_0 = (0.428 \pm 0.074)$ mK.

The energy per particle in the CNAF phase is given by Eqs. (17) and (18) with the values of the parameters calculated previously (26). Similar results for the U_2D_2 phase are given by expressions (22), (23), and (31).

The difference between the energy of the U_2D_2 phase and that of free spins at $T = 0$ and $B_0 = 0$ is therefore

$$E_L - E_0 = u - E_0 = (-\tfrac{1}{2}J_{2N} + 2T_1 - 2T_2 + \tfrac{3}{2}K_P$$

$$-\tfrac{1}{2}K_F - 2K_A - K_B - 5K_L$$

$$-\tfrac{5}{4}K_S - 3F + \tfrac{1}{4}S_1 + \tfrac{3}{4}S_2) \ . \qquad (35)$$

At melting density, $E_L - E_0 = -(0.664 \pm 0.036)$ mK. This value is close to that found in earlier calculations. With $T_1 = -0.167$ mK and $K_F = K_P = -0.264$ mK (Iwahashi, Miwa, and Masuda[19]) $E_L - E_0 = -0.598$ mK; with $J_{1N} = -0.377$ mK, $T_1 = -0.155$ mK, and $K_P = -0.327$ mK (Stipdonk and Hetherington[6]) $E_L - E_0 = -0.800$ mK; and for $T_1 = -0.130$ mK and $K_P = -0.385$ mK (Roger, Hetherington, and Delrieu[1]) $E_L - E_0 = -0.838$ mK. This quantity has been determined experimentally by Fukuyama *et al.*;[20,21] their value, (-1.24 ± 0.02) mK, is substantially larger in magnitude than the calculated one. This discrepancy is not surprising. Iwahashi and Masuda[22] and Roger, Delrieu, and Hetherington[1] calculated that the energy gain due to spin fluctuations is of the same order of magnitude as the mean-field value of the ground-state energy. Their conclusions are consistent with the present results. High-order exchange processes, however, will decrease the calculated energy of the U_2D_2 phase (see the discussion of Sec. IV A).

The energy of both phases is shown in Fig. 9. The energy of the U_2D_2 phase displays the classical parabolic dependence on the magnetic field. In low fields (< 1 T), it is approximately constant: $E_L \simeq u = (-0.237 \pm 0.092)$ mK. The energy of the CNAF phase is almost linear in magnetic field, since the magnetization is practically constant and equal to its zero-field value $m_0 = (0.54 \pm 0.05)$. It can be described in low fields, to a good approximation, as

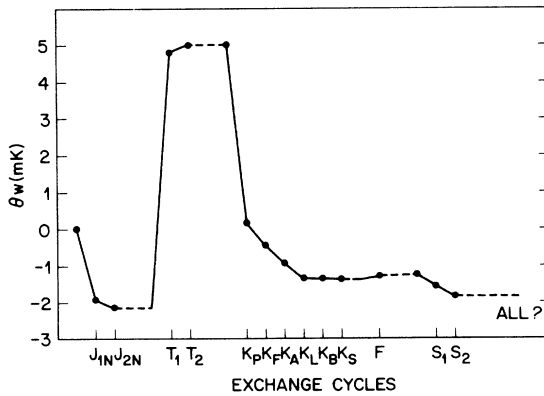$$E_H \simeq E_{H0} - \alpha B_0 \ ,$$

with

FIG. 8. Schematic representation of the predicted Curie-Weiss temperature as the number of exchange cycles considered is increased. Due to a substantial cancellation of terms with opposite signs, the final value is practically equal to the nearest-neighbor contribution.
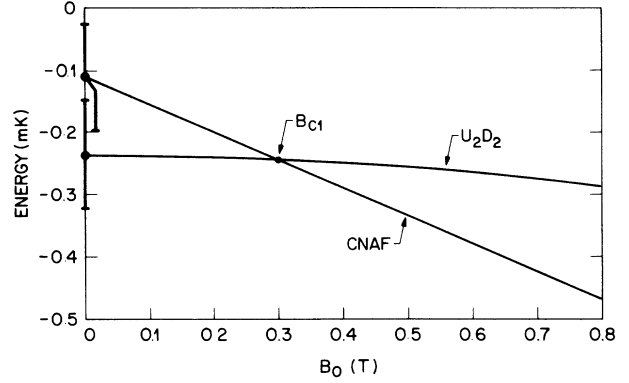

FIG. 9. The calculated energy of the CNAF and U_2D_2 phases at zero temperature, as a function of the magnetic field. The experimental value of the lower critical field B_{c1} is 0.451 T (Ref. 10). Note that the energy of free spins is 0.428 mK at zero field (see text).

$$E_H = a + bm_0^2 + cm_0^4 + dm_0^6 - \frac{\gamma \hbar}{2k_B} m_0 B_0 \ ,$$

and, numerically, as

$$E_H \simeq (-0.115 \pm 0.09) - (0.42 \pm 0.04)B_0 \ \text{mK} \ .$$

The difference of the energies of the two phases at zero field is $E_H - E_L = (0.122 \pm 0.13)$ mK, taking into account the fact that the errors are weakly correlated.

Therefore, the U_2D_2 phase is found to be the stable phase at zero field, but with a substantial uncertainty, which originates mainly from that on u and b.

The lower critical field is extremely sensitive to this uncertainty; equating E_L and E_H only allows one to state that $0 < B_{c1} < 0.8$ T. These results can be compared to the experimental values;[10]

$B_{c1} = (0.4513 \pm 0.0005)$ T, and the reduced magnetization at low fields $(\sim B_{c1})$ is $(0.595 \pm 0.0005)M_{sat} = m_{H1}$.

Within realistic approximations, $E_H = E_{H0} - \alpha B_0$ with $\alpha = \gamma \hbar m_{H1} / 2k_B = 0.463$ mK/T, and

$$E_L = E_{L0} - \tfrac{1}{2}B_0^2 V\chi / Nk_B\mu_0 = E_{L0} = 0.0788B_0^2 \ ,$$

where the energies per particle are in mK and B_0 in Tesla, and $\chi = 5.41 \times 10^{-6}$ (cgs) $= 6.80 \times 10^{-5}$ (mks).[10] The difference of energies of the U_2D_2 and CNAF phases at zero field and temperature is $E_{H0} - E_{L0} = \alpha B_{c1} - 0.0788B_{c1}^2 = (0.192 \pm 0.004)$ mK. This value is therefore very accurately determined by the experiment.[10] The theoretical result obviously agrees with the experiment, but with substantial error bars. A better theoretical determination of the exchange coefficients is clearly needed. It appears, however, that within the present accuracy (~ 0.1 mK) the reduction of the energy with respect to the mean-field value, due to spin fluctuations, is of the same order of magnitude (~ 0.6 mK) for both ordered phases, although some difference could be expected. Within the two-parameter model, this difference has been calculated[1] to be ~ 0.25 mK. A spin-wave cal-

culation similar to that given by Iwahashi and Masuda[22] should be performed including the exchange cycles considered here to determine the ground-state energy.

E. Conclusions

The multiple-spin-exchange Hamiltonian has been developed in terms of Pauli spin operators for an arbitrary number of particles in the exchange cycle. The properties of the ordered phases at absolute zero and the Curie-Weiss temperature in the paramagnetic phase have been calculated considering a large number of exchange cycles, using the exchange frequencies derived by Monte Carlo techniques by Ceperley and Jacucci.[7]

A good agreement is obtained between theory and experiment. It should be pointed out that the theory has no adjustable parameters. The description of the magnetic properties of the U_2D_2 phase is excellent, although corrections for quantum fluctuation have been neglected. In the high-field phase, however, some systematic discrepancies are observed. These could be due to higher-order exchange rings which contribute to high powers of the magnetization in the expansion of the energy. As discussed before, all coefficients are expected to be small but positive for high-order terms. The energy of the ordered phases, however, is reduced by zero-point spin fluctuations, not considered in the present calculation. This well-known limitation of the mean-field theory is compensated by the fact that the effect is of the same order in both phases.

The calculated properties of the paramagnetic phase are in good agreement with the experimental values (see Sec. IV C and Ref. 7). It is clear that the model gives an excellent description of the magnetic properties of solid ^{3}He. Some important questions are still open: the effect of spin fluctuations, of higher-order exchange processes, etc.

A more accurate Monte Carlo evaluation of the exchange parameters is certainly needed, since present uncertainties are larger than 10% for several exchange coefficients. It would also be desirable to have an evaluation of the exchange coefficients for eight nearest-neighbors rings; this would allow one to estimate the uncertainty associated with higher-order processes in the description of the high-field phase.

From the experimental point of view, investigations of the CNAF phase at very large magnetic fields, near the upper critical field B_{c2}, are clearly needed. Multiple-spin-exchange effects are easily identified in this phase.

It appears that the properties of the solid ^{3}He magnet can indeed be calculated from first principles, without any adjustable parameters; and although more work is needed, the success of the present description is certainly encouraging.

ACKNOWLEDGMENTS

[1]M. Roger, J. H. Hetherington, and J. M. Delrieu, Rev. Mod. Phys. 55, 1 (1983).

[2]M. C. Cross and D. S. Fisher, Rev. Mod. Phys. 57, 881 (1985).

[3]P. A. M. Dirac, The Principles of Quantum Mechanics (Clarendon, Oxford, 1947), Chap. IX.

[4]D. J. Thouless, Proc. Phys. Soc. London 86, 893 (1965); 86, 905 (1965).

[5]M. Roger, Phys. Rev. B 30, 6432 (1984).

[6]H. L. Stipdonk and J. H. Hetherington, Phys. Rev. B 31, 4684 (1985); M. C. Cross and R. N. Bhatt, ibid. 33, 7809 (1986).

[7]D. M. Ceperley and G. Jacucci, Phys. Rev. Lett. 58, 1648 (1987) [note that the frequency of 6(1^6; 3^6; 4^3) is 0.036 instead of 0.36 mK].

[8]D. D. Osheroff, M. C. Cross, and D. S. Fisher, Phys. Rev. Lett. 44, 792 (1980).

[9]A. Benoit, J. Bossy, J. Flouquet, and J. Schweitzer, J. Phys. Lett. (Paris) 46, L-923 (1985).

[10]D. D. Osheroff, H. Godfrin, and R. R. Ruel, Phys. Rev. Lett. 58, 2458 (1987).

[11]H. Godfrin, G. Frossati, A. S. Greenberg, B. Hebral, and D. Thoulouze, Phys. Rev. Lett. 44, 1695 (1980); H. Godfrin, thèse d'état, Universite de Grenoble, 1981.

[12]E. D. Adams, E. A. Schubert, G. E. Haas, and D. M. Bakalyar, Phys. Rev. Lett. 44, 789 (1980).

[13]D. D. Osheroff, Physica 109&110B, 1461 (1982).

[14]A. Sawada, H. Yano, M. Kato, K. Iwahashi, and Y. Masuda, Phys. Rev. Lett. 56, 1587 (1986).

[15]D. S. Greywall (unpublished).

[16]A. K. McMahan and R. A. Guyer, Phys. Rev. A 7, 1105 (1973).

[17]D. M. Ceperley (private communication).

[18]W. P. Kirk, Z. Oleiniczak, P. Kobiela, A. A. V. Gibson, and A. Czernmak, Phys. Rev. Lett. 51, 2128 (1983), and references therein.

[19]K. Iwahashi, Y. Miwa, and Y. Masuda, J. Phys. Soc. Jpn. 53, 3088 (1984).

[20]H. Fukuyama, A. Sawada, Y. Miwa, and Y. Masuda, in Proceedings of the 17th International Conference on Low Temperature Physics, edited by U. Eckern, A. Schmid, W. Weber, and H. Wühl, (North-Holland, Amsterdam, 1984), p. 275.

[21]H. Fukuyama, H. Ishimoto, T. Tazaki, and S. Ogawa (unpublished).

[22]K. Iwahashi and Y. Masuda, J. Phys. Soc. Jpn. 50, 2508 (1981).